



## Photocatalytic degradation of methyl orange using cerium doped zinc oxide nanoparticles supported bentonite clay

Safoura Javan<sup>a</sup>, Mohammad Reza Rezaei Kakhkha<sup>b\*</sup>, Fahimeh Moghaddam<sup>b</sup>,

Mohsen Faghihi-Zarandi<sup>c</sup>, and Anahita Hejazi<sup>d</sup>

<sup>a</sup> Departement of Environmental Health Engineering, Neyshabur University of Medical Sciences, Neyshabur, Iran

<sup>b</sup> Department of Environmental Health Engineering, Zabol University of Medical Sciences, Zabol, Iran

<sup>c</sup> Foreign Language Department, Shahid Bahonar University of Kerman, Kerman, Iran

<sup>d</sup> Engineering Department of Occupational Health & Safety at Work, Kerman University of Medical Sciences, Kerman, Iran

### ARTICLE INFO:

Received 3 Aug 2022

Revised form 20 Oct 2022

Accepted 17 Nov 2022

Available online 30 Dec 2022

### Keywords:

Photocatalyst,  
Degradation,  
Clay,  
Bentonite,  
Methyl Orange,  
Dye

### ABSTRACT

Methyl orange (MO) is a common anionic azo dye that is a serious harmful pollutant to the environmental aquatic systems, so it must be treated before it can be discharged. Photocatalysts are usually semiconducting solid oxides that create an electron-hole pair by absorbing photons. These electron holes can react with molecules on the surface of the particles. Photocatalysts are used in water purification, self-cleaning glasses, the decomposition of organic molecules, etc. Photocatalysts are environmental cleaning materials that remove pollution from surfaces and can destroy organic compounds when exposed to sunlight or fluorescence. The photocatalytic process follows the following principles. Bentonite mineral is a natural adsorbent material that has good adsorption capacity. In this work, zinc oxide nanoparticles doped with cerium were prepared by the sol-gel method (SGM) and deposited on bentonite clay to degrade methyl orange (MO) dye. Important parameters that affected degradation efficiency such as contact time, amount of nanocatalyst, and initial dye concentration were investigated and optimized. Results showed that 100% degradation efficiency was obtained at 60 mg of nanocatalyst and 50 mg L<sup>-1</sup> of methyl orange in 120 minutes. The Kinetics of the degradation process was consistent with pseudo-second-order and the adsorption isotherm of MO dye on nanocatalyst was fitted with the Langmuir isotherm model. The reusability of the synthesized nanocatalyst showed that the nanocatalyst was applied successfully seven times without a significant change in degradation efficiency.

### 1. Introduction

Photocatalysts are one of the essential elements for advanced oxidation processes (AOPs) [1, 2]. Zinc oxide (ZnO) is often the first choice due to its cheapness, non-toxicity, chemical stability, and high photocatalytic activity. Photocatalysts

absorb light radiation (ultraviolet or visible) by the catalyst, and electrons are transferred from the semiconductor's valence band to the conduction band. This transition creates a hole in the valence band, and an electron is produced in the conduction band (**Schema 1**).

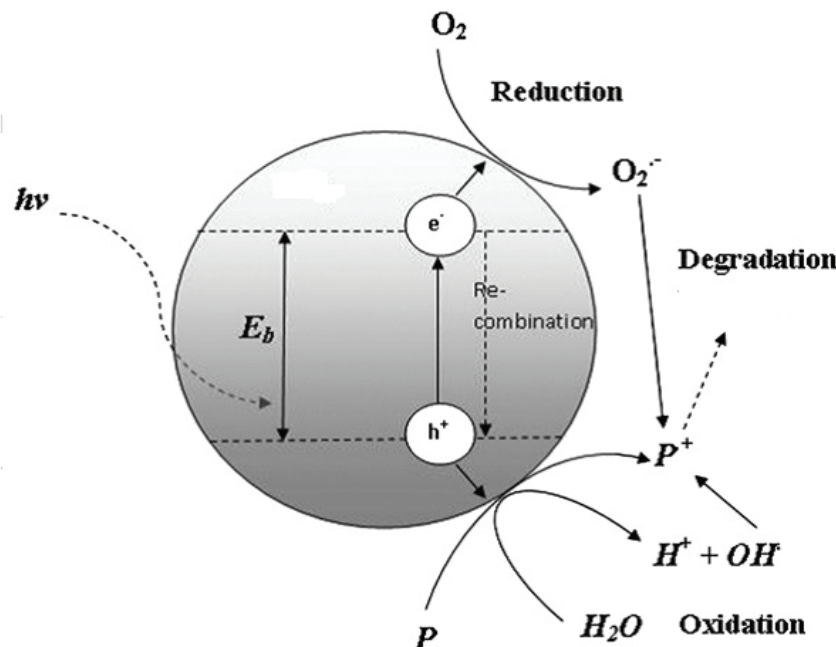
The hole in the reaction with water molecules produces active hydroxyl radicals [3, 4].

Moreover, the produced electron is transferred to the dissolved oxygen and forms a superoxide

\*Corresponding Author: Mohammad Reza Rezaei Kakhkha

Email: [m.r.rezaei.k@gmail.com](mailto:m.r.rezaei.k@gmail.com)

<https://doi.org/10.24200/amecj.v5.i04.216>



**Schema 1.** Photocatalytic process

radical. These radicals can remove pollutants in aqueous media. Since the produced electron and holes are unstable and can recombine and return to their original state, doping elements were used with ZnO to prevent these phenomena[5]. Cerium is one of the elements of the lanthanide family whose redox couple Ce (III)/Ce (IV) causes the production of  $\text{CeO}_2$  and  $\text{Ce}_2\text{O}_3$  oxides. Ce (IV) traps the electron created in the conduction band, which has lost its stable electron configuration, tends to donate its electron and become stable, which is possible by electron migration to oxygen absorbed on the surface and the formation of superoxide radicals. Therefore, the electron of the conduction band enters a new cycle, which reduces the possibility of its access to the hole[6, 7]. Despite the advantages of nanocatalysts, their use in water purification processes is limited due to the small size of the particles. Problems such as the separation of suspended particles, non-recycling and secondary pollution are among the limitations of this method. One proposed method to solve this problem is fixing nanocatalysts on suitable substrates[8]. Many researchers developed different types of substrates such as silica gel[9], activated carbon [10], stainless steel

[11], glass fibers [12] and wood foam [13], has been used. Recently, ZnO nanoparticles were immobilized on cellulose paper [14], which was used to treat textile wastewater in a photoreactor. Natural clays such as bentonite, montmorillonite, and perlite are used as catalyst substrates due to their high porosity, chemical inertness, non-degradability, and high mechanical and thermal resistance compared to the other mentioned substrates[15]. In this work, ZnO-Ce nanoparticles were first synthesized by the sol-gel method. Then, nanoparticles were fixed on bentonite. The performance of the synthesized nanocatalyst as a catalyst was investigated in the removal of methyl orange in a batch photoreactor.

## 2. Material and methods

### 2.1. Reagents and instrumental

All reagents and chemicals are analytical grade and used as received. Zinc acetate dihydrate  $\text{Zn}(\text{CH}_3\text{COO})_2 \cdot 2\text{H}_2\text{O}$ ; CAS Number: 5970-45-6), cerium (CAS Number: 7440-45-1), nitrate (SRM from NIST:  $\text{NaNO}_3$  in  $\text{H}_2\text{O}$  1000  $\text{mgL}^{-1}$   $\text{NO}_3^-$ , Sigma), hydrochloric acid (CAS Number: 7647-01-0), sodium hydroxide (CAS Number: 1310-73-2), absolute ethanol (CAS Number: 64-17-5) and MO

dye (Content 85 %; CAS Number: 547-58-0; EC Number: 208-925-3; Sigma) were obtained from Sigma and Merck (Germany). Bentonite (CAS Number: 1302-78-9) was purchased from Sigma (Sigma, USA). The pH of the solutions was adjusted using a Metrohm (Metrohm, Switzerland) pH meter. The color concentration was measured using a double beam-UNICO 4802 spectrophotometer at its maximum wavelength (584 nm). FTIR spectrum was recorded by Bruker Tensor 27 device.

## 2.2. Synthesis of ZnO-Ce nanoparticles

The sol-gel method was used to prepare ZnO-Ce nanoparticles. First, 8.5 mL of zinc acetate was added to 40 mL of absolute ethanol and the solution was placed in an ultrasonic bath for 30 minutes (Solution A). Then 0.12 g of cerium nitrate was dissolved in 20 mL of absolute ethanol and 3 mL of deionized water and 2 mL of hydrochloric acid were added to it. Then, the solution was placed in an ultrasonic bath for 10 minutes (solution B). Solution B was added drop by drop to solution A while stirring to form a gel. To evaporate the ethanol, the gel was placed in an oven with a temperature of 80°C for 12 hours and then calcined for 3 hours in an oven at a temperature of 550°C.

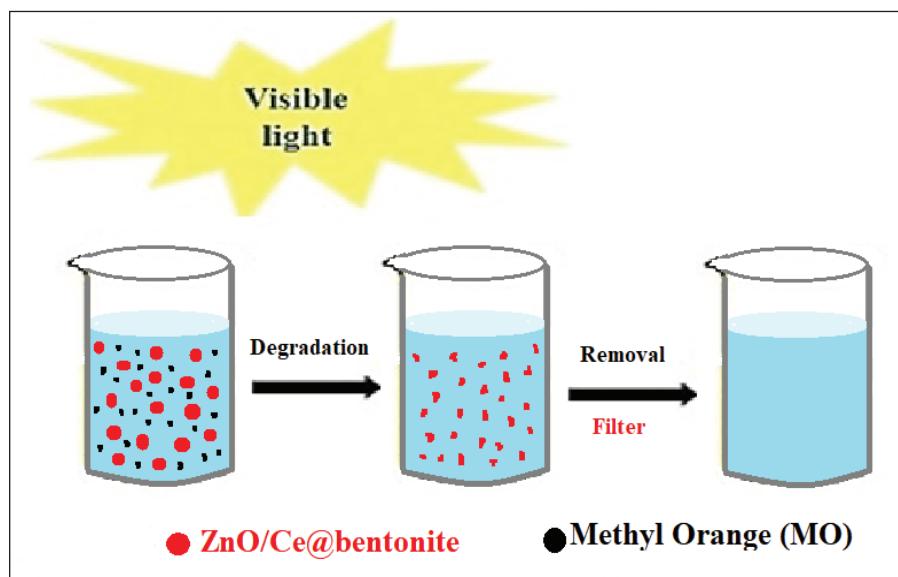
## 2.3. Synthesize bentonite nanocatalyst

The immersion method was used to synthesize

bentonite nanocatalysts coated with ZnO-Ce nanoparticles. For this purpose, 0.1 g of ZnO-Ce nanoparticles was added to one liter of ethanol and water with a ratio of 3:1. For homogenization, the slurry solution was placed in an ultrasonic bath (35 kHz, 40 W) for 30 minutes. Next, bentonite was immersed in the solution for one minute. Then the bentonite was first dried at room temperature and then dried in an oven at 80°C for 2 hours. To increase the adhesion of nanoparticles to the surface of bentonite, the granular bentonite was heated in an oven at a temperature of 550°C for 2 hours.

## 2.4. Removal procedure

Photocatalytic removal of MO by ZnO-Ce nanoparticles was studied using a batch reactor, equipped with a UVC lamp at room temperature (25 °C). To enhance removal efficiency, the reactor was covered with aluminum sheets. The appropriate dose of ZnO nanoparticle was mixed with different amounts of MO dye. The solution was stirred at 300 rpm for 30 minutes while the UV lamp at 3800 W irradiated the solution. After the experiment, 30 ml of the sample was taken and in order to separate the zinc oxide nanoparticles, the sample was centrifuged at 5000 rpm and filtered. Remind concentration was measured by spectrophotometer at 530 nm (**Schematic 2**) shows the diagram of degradation of MO).



**Schema 2.** Schematic diagram of degradation of MO

The removal percentage of MO dye (%removal) was calculated as [Equation 1](#).

$$\% Removal = \frac{C_{eq} - C_0}{C_0} * 100$$

(Eq.1)

Parameters affecting the removal of MO dye, including the amount of the nanocomposite (10–100 mg), initial concentration of MO dye (25–150 mg L<sup>-1</sup>), and contact time (30–210 min), were investigated.

### 3. Results and discussion

#### 3.1. Characterization of nanocatalyst

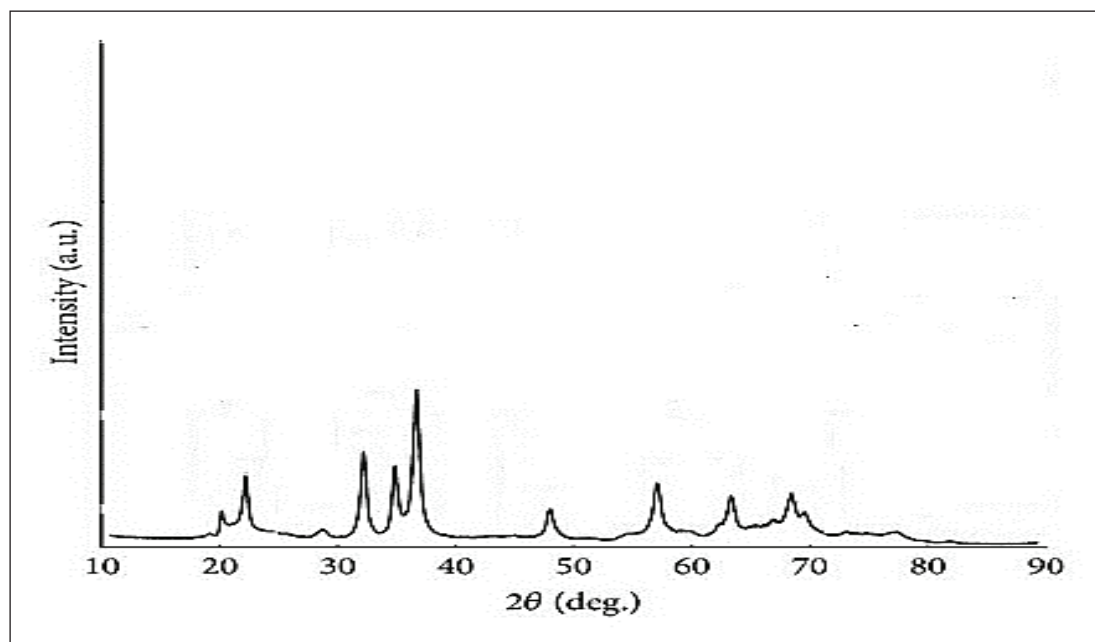
##### 3.1.1. XRD pattern of ZnO/Ce/bentonite

[Schematic 3](#) showed an XRD pattern of the

synthesized nanocomposite. It can be seen in [schema 3](#) that by doping cerium as an impurity, the peaks related to the rutile phase are removed and only the anatase phase is observed. In other words, the presence of cerium as an impurity greatly improves the growth of anatase phase crystals and prevents the transfer of the anatase phase to rutile.

#### 3.1.2. SEM image of synthesized ZnO/Ce/bentonite

[Schematic 4](#) showed an SEM image of a synthesized nanocatalyst. It can be concluded that the presence of cerium in the ZnO structure reduces the size of nanoparticles. Considering the strong dependence of the properties of nanoparticles on their size, we can expect significant changes in the properties of ZnO/Ce/bentonite nanoparticles.



**Schema 3.** XRD pattern of ZnO/Ce adsorbent

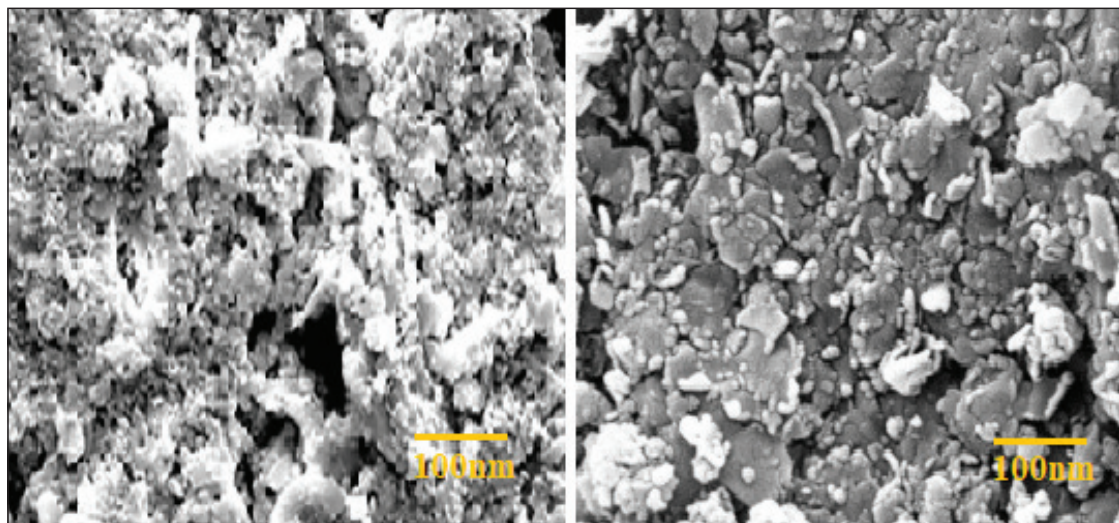
### 3.2. The optimized parameters for photocatalytic removal of MO

#### 3.2.1. Effect of amount of nanocatalyst

The amount of ZnO /Ce / bentonite nanocatalyst impacts the adsorption of the MO dye. The removal efficiency and the adsorption capacity were investigated. For this purpose, experiments were conducted using an adsorbent dosage in the range of 10 to 120 mg. As depicted in Figure 1, the uptake of the MO dye was significantly increased, up to 60 mg. Furthermore, by increasing the amount of nanocatalyst, the removal efficiency was increased.

#### 3.2.2. Effect of initial concentration of MO dye on removal efficiency

The effect of the initial concentration of dye on removal percentage by ZnO/Ce/Bentonite nanocatalyst was investigated in the range of 20 to 150 mg L<sup>-1</sup>. The result is shown in Figure 2. In the early stages of adsorption, the results showed a significant increase. The maximum percent removal was achieved at 50 mg L<sup>-1</sup> of MO dye. After this point, the saturation of active sites on the nanocatalyst has occurred, resulting decrease in the adsorbent's ability to the sorbent.



**Schema 4.** SEM image of synthesized adsorbent

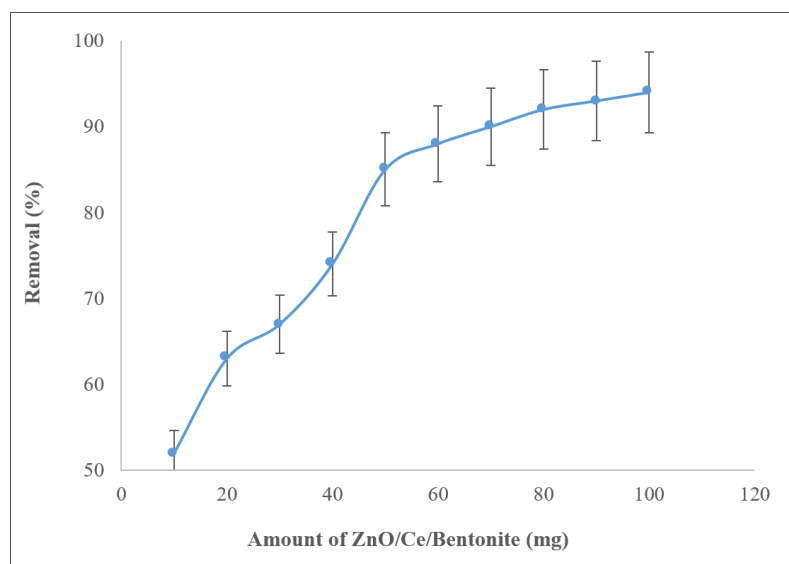


**Fig. 1.** Effect of ZnO/Ce/Bentonite amount on degradation efficiency

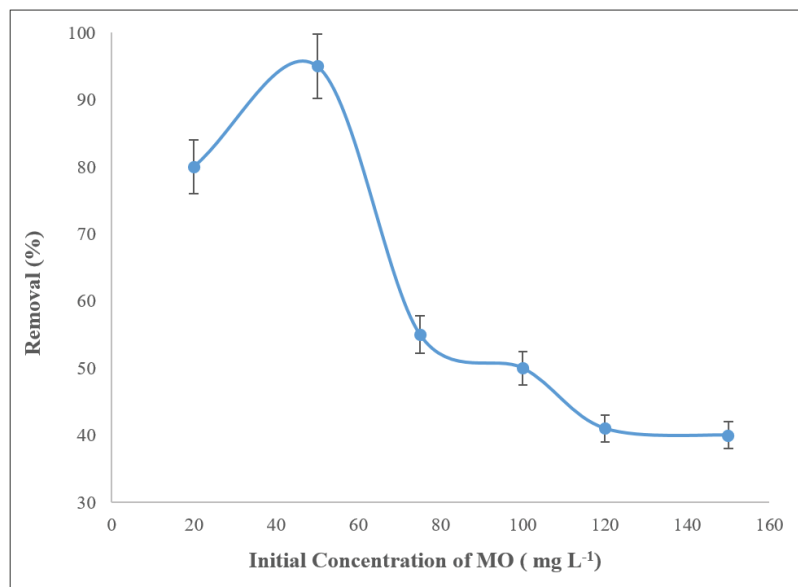


**Fig. 2.** Effect of dye concentration on degradation efficiency

### 3.2.3. Effect of time on degradation efficiency

The effect of contact time on the degradation efficiency of MO dye by ZnO/ Ce/ Bentonite nanocatalyst was investigated. The results are depicted in Figure 3. The removal percentages of MO dye increased significantly in the early stages. After a while, the percentage degradation will rise slightly until an equilibrium is reached. The results showed that the best dye removal percentage was obtained at 120 minutes. Hence, this time was selected for subsequent experiments.

### 3.2.4. Kinetic study

Adsorption kinetic studies of MO dye onto ZnO/ Ce/ Bentonite nanocatalyst were investigated using pseudo-first-order and pseudo-second-order kinetics. The results are shown in Figure 4 and summarized in Table 1. The kinetic model that best fits the adsorption of MO dye on the nanocatalyst was determined by  $R^2$  values. Considering the reported  $R^2$  values, the adsorption of MO dye on ZnO/ Ce/ Bentonite nanocatalyst was followed by a pseudo-second-order kinetics model.

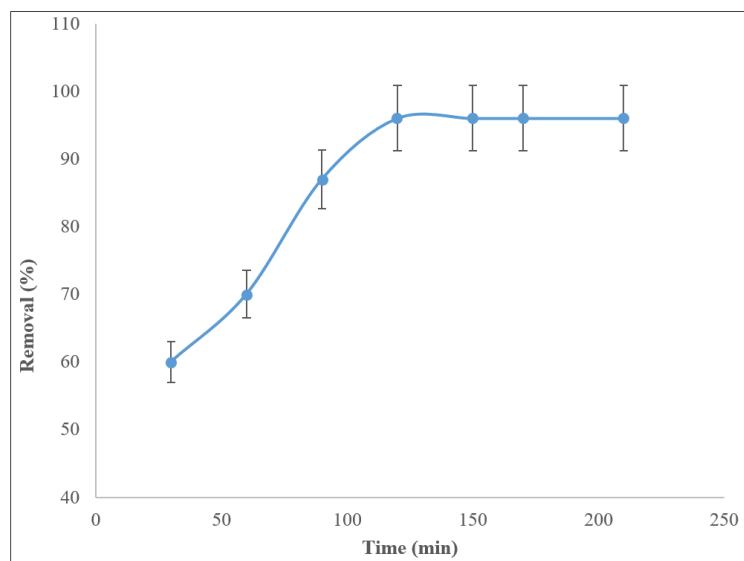


**Fig. 3.** Effect of time on degradation efficiency

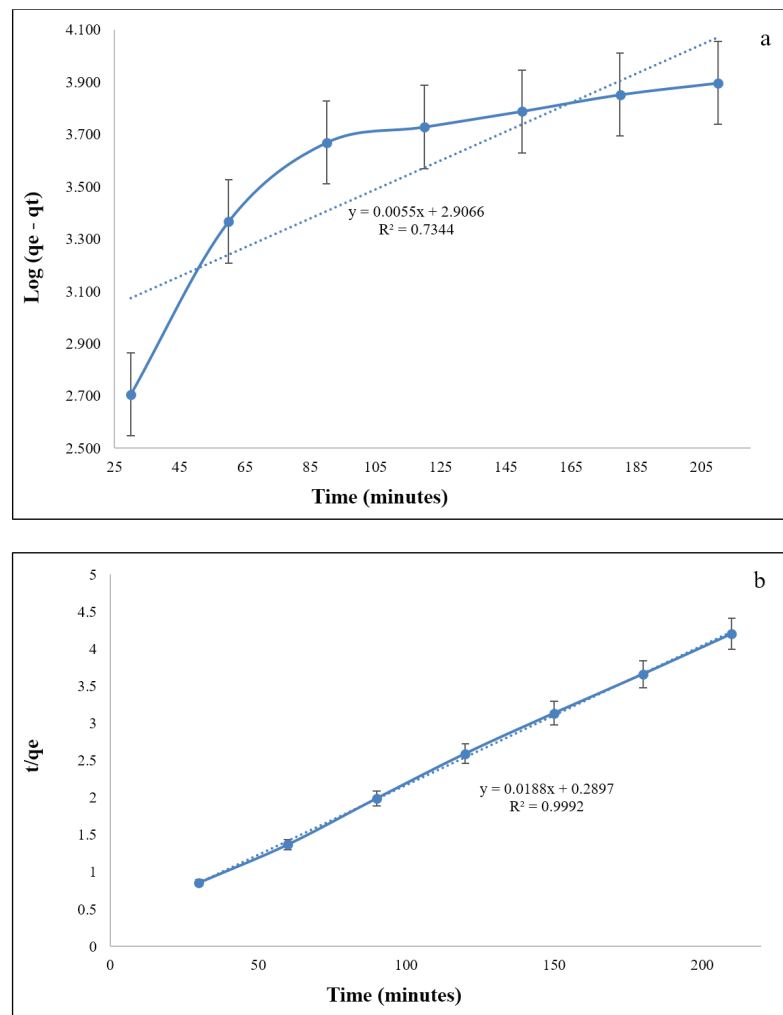


**Fig. 4.** Kinetic studies of the adsorption of MO dye on nanocatalyst.

a) Psuedo First order    b) Psuedo second order

**Table 1.** Kinetics parameters for MO dye

MO dye	First order kinetics		Second order kinetics	
	R <sup>2</sup>	K <sub>1</sub> (min <sup>-1</sup> )	R <sup>2</sup>	K <sub>1</sub> (g.mg <sup>-1</sup> min <sup>-1</sup> )
	0.8344	-6.51X10 <sup>-3</sup>	0.9992	1.88X10 <sup>-2</sup>

### 3.2.5. Adsorption isotherms

For the evaluation of adsorption isotherms, Langmuir and Freundlich's isotherms were used to illustrate the mechanism. The Langmuir and Freundlich isotherms for MO dye on nanocatalyst were depicted in Figure 5 and Table 2. It was found that the adsorption of Mo dye on ZnO/Ce/Bentonite nanocatalyst followed from Langmuir isotherm.

### 3.2.6. Reusability of Nanocatalyst

Evaluating the reusability of ZnO/Ce/Bentonite nanocatalyst on the degradation of MO dye photocatalytic experiments in optimal conditions was repeated several times. Afterward, the nanocatalyst was washed, dried, and reused for the next run. Results showed that degradation efficiency was decreased from 100 to 98.1 after 7 repeated experiments that confirmed the reusability of the nanocatalyst. Also, for the evaluation of the

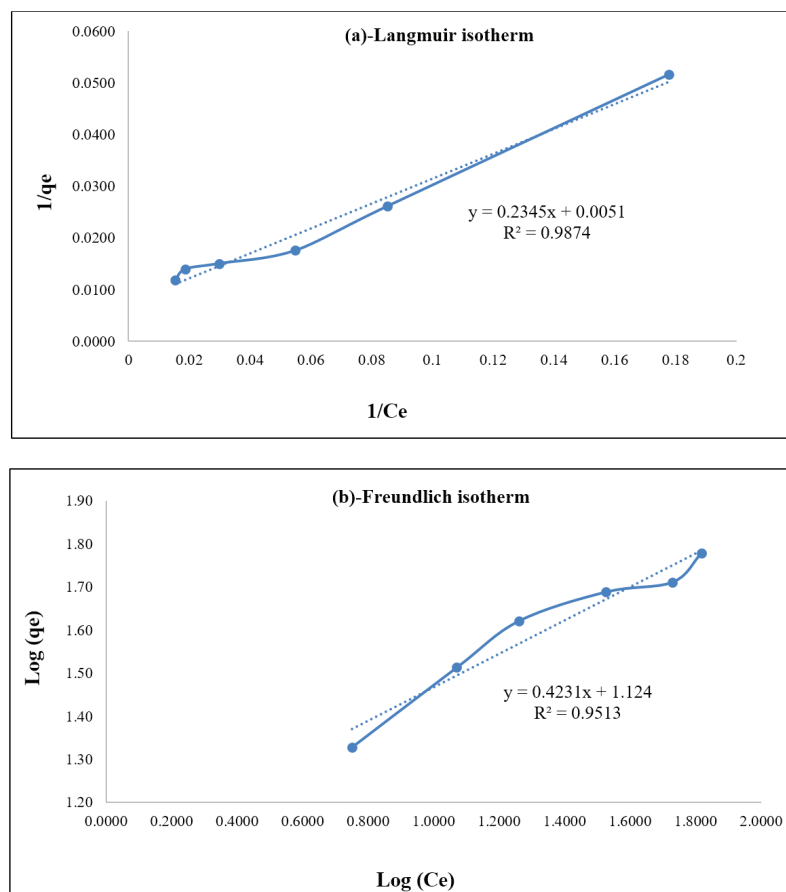


**Fig. 5.** a) Langmuir isotherm of MO dye onto nanocatalyst,  
b) Freundlich isotherm of MO dye onto nanocatalyst

**Table 2.** Isotherms parameter of MO dye

MO dye	Langmuir		Freundlich	
	R <sub>L</sub>	K <sub>L</sub>	K <sub>F</sub>	N
Results	0.9874	0.3989	0.03345	0.9513
			11.9674	2.5713

sorption capacity of the nanocatalyst, a standard solution containing  $100 \text{ mg L}^{-1}$  of MO was applied. The initial and final amounts of MO dye were determined by spectrophotometer after adsorption on ZnO/Ce/ Bentonite. The maximum adsorption capacity was defined as the total amount of adsorbed MO per gram of the nanocatalyst. The obtained capacity was found to be  $115 \text{ mg g}^{-1}$ .

#### 4. Conclusion

The degradation efficiency of methyl orange using ZnO/Ce/Bentonite nanocatalyst as photocatalyst and adsorbent was investigated. The optimal conditions

for the degradation efficiency of the dye were found at a nanocatalyst dosage of  $60 \text{ mg}$ , a contact time of  $120 \text{ min}$  yellow. At optimum conditions,  $100\%$  of methyl orange was removed by synthesized nanocomposite. Also, the nanocatalyst was reused after 7 repeated cycles, and adsorption capacity was obtained  $115 \text{ mg g}^{-1}$ . The isotherm data of MO dye were fitted with the Langmuir model, while the kinetic data were modeled by the pseudo-second-order, revealing that the nature of the kinetic adsorption is chemical. The present study showed that the ZnO/ Ce/ Bentonite nanocatalyst is an effective adsorbent for the degradation of MO dye from aqueous solutions.

## 5. Acknowledgements

Authors at this moment thank from health laboratory of Zabol University for their cooperation to perform experiments.

## 6. References

- [1] A. Rafiq, M. Ikram, S. Ali, F. Niaz, M. Khan, Q. Khan, M. Maqbool, Photocatalytic degradation of dyes using semiconductor photocatalysts to clean industrial water pollution, *J. Ind. Eng. Chem.*, 97 (2021) 111-128. <https://doi.org/10.1016/j.jiec.2021.02.017>
- [2] B. Viswanathan, Photocatalytic degradation of dyes: an overview, *Curr. Catal.*, 7 (2018) 99-121. <http://dx.doi.org/10.2174/2211544707666171219161846>
- [3] J. Singh, Biogenic synthesis of copper oxide nanoparticles using plant extract and its prodigious potential for photocatalytic degradation of dyes, *Environ. Res.*, 177(2019) 108569. <https://doi.org/10.1016/j.envres.2019.108569>
- [4] S. Alkaykh, A. Mbarek, E.E. Ali-Shattle, Photocatalytic degradation of methylene blue dye in aqueous solution by MnTiO<sub>3</sub> nanoparticles under sunlight irradiation, *Heliyon*, 6 (2020) e03663. <https://doi.org/10.1016/j.heliyon.2020.e03663>
- [5] L. Yang, Three-dimensional bacterial cellulose/polydopamine/TiO<sub>2</sub> nanocatalyst membrane with enhanced adsorption and photocatalytic degradation for dyes under ultraviolet-visible irradiation, *J. Colloid Interface Sci.*, 562 (2020) 21-28. <https://doi.org/10.1016/j.jcis.2019.12.013>
- [6] H. Chaker, A statistical modeling-optimization approach for efficiency photocatalytic degradation of textile azo dye using cerium-doped mesoporous ZnO: A central composite design in response surface methodology, *Chem. Eng. Res. Des.*, 171 (2021) 198-212. <https://doi.org/10.1016/j.cherd.2021.05.008>
- [7] R. Jasrotia, Photocatalytic degradation of environmental pollutant using nickel and cerium ions substituted Co<sup>0.6</sup>Zn<sub>0.4</sub>Fe<sub>2</sub>O<sub>4</sub> nanoferrites, *Earth Syst. Environ.*, 5 (2021) 399-417. <https://doi.org/10.1016/j.jece.2018.09.029>
- [8] A. Mohammad, Adsorption promoted visible-light-induced photocatalytic degradation of antibiotic tetracycline by tin oxide/cerium oxide nanocatalyst, *Appl. Surface Sci.*, 565 (2021) 150337. <https://doi.org/10.1016/j.apsusc.2021.150337>
- [9] M.R. AbuKhadra, Enhanced photocatalytic degradation of acephate pesticide over MCM-41/Co<sub>3</sub>O<sub>4</sub> nanocatalyst synthesized from rice husk silica gel and Peach leaves, *J. Hazard. Mater.*, 389 (2020) 122129. <https://doi.org/10.1016/j.apsusc.2021.150337>
- [10] M.S. Nasrollahzadeh, Synthesis of ZnO nanostructure using activated carbon for photocatalytic degradation of methyl orange from aqueous solutions, *Appl. Water Sci.*, 8 (2018) 1-12. <https://doi.org/10.1007/s13201-018-0750-6>
- [11] J. Singh, A. Dhaliwal, Electrochemical and photocatalytic degradation of methylene blue by using rGO/AgNWs nanocatalyst synthesized by electroplating on stainless steel, *J. Phys. Chem. Solids*, 160 (2020) 110358. <https://doi.org/10.1016/j.jpcs.2021.110358>
- [12] S. Fukugaichi, Fixation of titanium dioxide nanoparticles on glass fiber cloths for photocatalytic degradation of organic dyes, *ACS omega*, 4 (2019) 15175-15180. <https://doi.org/10.1021/acsomega.9b02067>
- [13] Z. Wang, Efficient and sustainable photocatalytic degradation of dye in wastewater with porous and recyclable wood foam@ V<sub>2</sub>O<sub>5</sub> photocatalysts, *J. Clean. Prod.*, 332 (2022) 130054. <https://doi.org/10.1016/j.jclepro.2021.130054>
- [14] S. Li, Promoting effect of cellulose-based carbon dots at different concentrations on multifunctional photocatalytic degradation of dyes by ZnO, *Opt. Mater.*, 121(2021) 111591. <https://doi.org/10.1016/j.optmat.2021.111591>
- [15] A. Mishra, A. Mehta, S. Basu, Clay supported TiO<sub>2</sub> nanoparticles for photocatalytic degradation of environmental pollutants: A review, *J. Environ. Chem. Eng.*, 6 (2018) 6088-6107. <https://doi.org/10.1016/j.jece.2018.09.029>

doi.org/10.1007/s41748-021-00214-9